Electronic Supplementary Material (ESI) for Nanoscale.

Supporting Information

Flexible Pressure Sensors with a Highly-Sensitive Layer to the Pressure and Strain Based on Nitroxyl Radical Grafted Hollow Carbon Sphere

*Jie Chu ,[a] Jueping Cai ,[*a]*

[a] School of Microelectronics, State key discipline laboratory of wide band gap semiconductor technology, Xidian University, Xi'an, 710071, China. Email: jpcai@mail.xidian.edu.cn

Note1. Experimental section

1.1 *Preparation of Hollow Carbon Sphere (HCSs)*

Step 1

In a typical synthesis method, a monodisperse silica sphere with a particle size close to 200 nm was synthesized by a modified stober method. First, tetraethoxysilane (TEOS) was vacuum distilled, and then 9 mL of TEOS was mixed with 100 mL of absolute ethanol (EtOH) and stirred at room temperature for 50 min to prepare a solution A. Solution B was prepared by mixing 6.8 mL of an aqueous ammonia solution (NH_4OH, 25 wt%), 22 ml of absolute ethanol (EtOH), and 38 mL of deionized water (H_2O). Stir at room temperature for 50 min and stir at high speed for 4 h. Add solution B to solution A quickly. The precursors were collected by centrifugation (3 times with deionized water and 2 times with absolute ethanol), and finally dried under vacuum at 50 ℃ for 24 h.

Step 2

First, 170 mg of 2-amino-2-hydroxymethylpropane-1,3-diol (Tris), 260 mg of triblock copolymer PEO-PPO-PEO (P123), and 500 mg of 200 nm monodisperse dioxide The silica spheres were dissolved in 170 mL of deionized water and stirred vigorously at room temperature for 10 h. Then, 300 mg of dopamine hydrochloride was dispersed in the mixed solution, and stirred at room temperature for 40 h. The particles were separated by centrifugation and washed 3 times with deionized water and 2 times with absolute ethanol, and then dried under vacuum at 50 ℃ for 24 hours. After that, the dried particles were heated in an Ar atmosphere at 400 ℃ at a heating rate of 1 ℃ min^{-1} for 3 h, and then further calcined at 800 ℃ for 5 h (a heating rate of 5 ℃ min^{-1}) . Finally, the powder was immersed in 8% HF solution and etched at 20 ℃ for 10-12 hours. The final product of HCSs was collected by centrifugation (washed 3 times with deionized water and 2 times with absolute ethanol), and vacuum drying was performed at 24 ℃ for 24 h to obtain a hollow carbon sphere HCSs.[1-4]

1.2 *Preparation of high concentration of carboxylated Hollow Carbon Sphere (HCS-g-COOH)*

In a typical synthesis method, 1.1 g of HCSs is first added to 76.0 mL of condensed H_2SO_4 (98 wt%), And then 3.2 g of $KMnO_4$ is added. A sealing film was used to prevent H_2SO_4 from coming into contact with moisture in the air, and the suspension was mechanically stirred for 6 days to ensure complete reaction with H_2SO_4. Then, 8.0 mL of deionized water was added 10 times every 5 min to raise the temperature to about 70 ℃. Finally, since the concentration of H2SO4 was less than 70 wt% after a short time, 150.0 mL of water was added to stop the

oxidation and it would lose its oxidizing ability. The suspension was continuously stirred for 48 h until the temperature was below 30 ℃, and after adding 13.0 mL of H_2O_2 (30 wt%), low-speed centrifugation and washing with deionized water to obtain clean HCS-*g*-COOH.[5-10]

1.3 *Preparation of high concentration of NO-radical Hollow Carbon Sphere (HCS-g-NO·)*

170 mL of the HCS-g-COOH dispersion was added to a dry round bottom flask, and 80 mL of thionyl chloride ($SOCl_2$) and 2 mL of anhydrous dimethylformamide (DMF) were added thereto, and the mixture was refluxed Stir at 70 ℃ for 48 hours. After the reaction was completed, it was filtered through a 0.22 μm organic phase filter, washed with anhydrous tetrahydrofuran (THF), and dried in a vacuum oven at 25 ℃ to HCS-*g*-COOH (acyl chloride). Then, 50 mL of THF, 1.27 g of 4-hydroxy-2,2,6,6-tetramethylpiperidine-1-oxy (HTEMPO), and 113.3 mg of dimethylaminopyridine (DMAP)) And 1.2 mL of triethylamine (Et_3N) and protected with nitrogen, while ensuring that the reaction temperature of the mixture is lower than 5 ℃.

After adding HCS-g-COOH (acyl chloride), the mixture was stirred at 0 ℃ for 8 hours, then heated to 70 ℃ and refluxed for 60 hours, and the reaction solution gradually changed from brown to black.

Finally, the suspension was filtered through a 0.22 μm filter membrane, washed 3-5 times with THF, 5 times with deionized water, and the product was dried under vacuum at 25 ℃. for 12 hours to obtain the product HCS-g-NO·.[11,12]

1.4 *Preparation of HCS-g-NO·@PDMS*

First, 200 mg of HCS-g-NO· was added to chloroform (7 mg/mL), and ultrasonic dispersion (150 W) was performed for 1 h to obtain a black suspension. Then, 1.2 g of PDMS was added to chloroform (500 mg/mL), and stirred with a magnetic stirrer at 1150 r / min for 1 h to obtain a PDMS diluted solution. Finally, the two solutions were mixed and ultrasonically dispersed to obtain a HCS-*g*-NO·@ PDMS @ chloroform suspension. This suspension was placed in a water bath at 55 ° C, and distilled under reduced pressure to volatilize chloroform. This temperature accelerates the volatilization rate of chloroform and prevents HCS-*g*-NO· agglomeration. After chloroform volatilizes, add PDMS curing agent (mass ratio, prepolymer: curing agent = 10:1), stir well and evacuate, pour into the mold to heat and solidify to obtain 1 cm × 1 cm HCS-*g*-NO·@PDMS composite film.[13]

1.5 *Materials characterization*

The prepared HCS-*g*-NO· powders were also observed using scanning electron microscopy (SEM, QUANTA FEG 250 equipped with an energy dispersive spectrometer). The

crystal structure of HCS-*g*-NO· was characterized by powder X-ray diffraction (X'Pert PRO MPD), and the XRD data were collected at a scan rate of 1° min^{-1} in the 2θ range of 10-60°. TEM and high-resolution transmission electron microscopy (FEI TECNAI G2 T20). Raman analysis was measured with a Renishaw (RM200) in Via micro-Raman system with a 532/633 nm laser. Using Fourier transform infrared spectroscopy instrument (FTIR, IRAffinity-1, SHIMADZU) detect the "N-O•" oxygen-containing functional groups on HCS-*g*-NO·. Electron spin resonance (ESR) spectra were obtained using a JEOL JES-TE200 ESR spectrometer with 100 kHz field modulation. X-ray photoelectron spectroscopy (XPS, VG ESCALAB MK II) was performed to determine the degree of carbon, oxygen, nitrogen and elemental composition of the obtained materials.

Note2. Measurement techniques for resistance versus pressure and tensile data

2.1 *The resistivity measurement procedure*

HCS-*g*-NO·@PDMS composites with different mass fractions were deposited on PCB with six elongated electrodes and leveled and cured by heating as shown in Supplementary Fig.S7. The resistivity measurement was based on the four-probe method. Six equally spaced parallel electrodes can be tested in three sets of four electrodes. Apply the sample through Tektronix DMM4040 digital multimeter at a voltage of -20V ~ 20V, the voltage increases by 0.1 volts every 0.5s.

2.2 *The resistivity measurement procedure*

A home-made force equipment was used to test the pressure response of the sensor as shown in Figure S8a. The sensor was applied the tensile and compressive strain through bending strain method, as shown in Figure S8b. The sensor was fixed at two ends by clamps and pushed in the middle to bend it. The strains induced by the deformations can be expressed as follows[14]:

$$\varepsilon = t / 2R \quad \backslash * \text{ MERGEFORMAT (1)}$$

where *t* is the sensor thickness and *R* is the radius of curvature of the membrane which is bent uniformly. Considering the geometric relationship in Figure S7b, *R* can be calculated as follow:

$$R^2 = \left(l / 2\right)^2 + (R - d)^2 \quad \backslash * \text{ MERGEFORMAT (2)}$$

where *l* can be measured easily and d can be read from fore equipment.

Note3. Sensitive mechanism modelling

The sensor follows Hooke's law: $R=\rho \cdot l/s=\rho \cdot G$, where G is the geometric coefficient. The sensitive layer is compressed under external pressure, and the conductive network changed, that is, both ρ and G change. Assume that the composite is an ideal elastomer, the following holds:

$$\frac{1}{G} \cdot \frac{\partial G}{\partial P} = -\frac{1+2\nu}{E} \quad \text{* MERGEFORMAT (3)}$$

where v denotes the Poisson coefficient, the E denotes elastic modulus and the P is pressure. After integrating formula (1), we have:

$$G = G_o \cdot e^{-\frac{1+2\nu}{E}P} \quad \text{* MERGEFORMAT (4)}$$

The conductive mechanism of conductive particle filled composites conforms to the effective medium model[15]:

$$\frac{(1-\varphi)(\rho_{PDMS}^{-\frac{1}{t}} - \rho^{-\frac{1}{t}})}{\rho_{PDMS}^{-\frac{1}{t}} + (1-\varphi_c)/\varphi_c \cdot \rho^{-\frac{1}{t}}} + \frac{\varphi(\rho_{HCS}^{-\frac{1}{t}} - \rho^{-\frac{1}{t}})}{\rho_{HCS}^{-\frac{1}{t}} + (1-\varphi_c)/\varphi_c \cdot \rho^{-\frac{1}{t}}} = 0 \quad \text{* MERGEFORMAT (5)}$$

where φ is filling concentration ($\varphi=V_{HCS}/V$), φ_C is the percolation threshold fraction and t is the percolation coefficient. HCS is assumed to be rigid (V_{HCS} remains constant with pressure) and uniformly distributed in the ideal elastomer, which is expressed as:

$$\frac{1}{\varphi} \cdot \frac{d\varphi}{dP} = \frac{1}{V_{HCS}} \frac{\partial V_{HCS}}{\partial P} - \frac{1}{V} \frac{\partial V}{\partial P} = -\frac{1}{V} \frac{\partial V}{\partial P} = -\frac{2\nu - 1}{E} \quad \text{* MERGEFORMAT (6)}$$

By integrating the formula (4), we can derive:

$$\varphi = \varphi_o \cdot e^{\frac{1-2\nu}{E}P} \quad \text{* MERGEFORMAT (7)}$$

So, the resistivity is:

$$\rho = \rho_{PDMS} \cdot (1-\varphi_c)^t \cdot (\varphi_o \cdot e^{\frac{1-2\nu}{E}P} - \varphi_c)^t \quad \text{* MERGEFORMAT (8)}$$

and the resistance is：

$$\frac{R}{R_o}=\frac{\rho\cdot G}{\rho_o\cdot G_o}=(\varphi_o-\varphi_c)^t[\varphi_o\cdot e^{\frac{1-2\nu}{E}P}-\varphi_c]^{-t}\cdot e^{-\frac{1+2\nu}{E}P} \quad \text{*}$$

MERGEFORMAT (9)

We differentiate the formula (7) and obtain the sensitivity relationship as follow:

$$S_R=\frac{|dR|}{R_o dP}=\frac{G|d\rho|}{\rho_o G_o dP}+\frac{\rho|dG|}{\rho_o G_o dP}=\frac{G}{G_o}\cdot\frac{|d\rho|}{\rho_o dP}+\frac{\rho}{\rho_o}\cdot\frac{|dG|}{G_o dP}=\frac{G}{G_o}\cdot S_\rho+\frac{\rho}{\rho_o}\cdot S_G \quad \text{*}$$

MERGEFORMAT (10)

where S_R, S_ρ, S_G are output resistance sensitivity, resistivity sensitivity and geometric sensitivity, respectively. When the pressure is in a small range, the sensitive mechanism mainly depends on the change in resistivity, and the pressure continues to increase, the sensitivity is close to the film deformation effect. The sensitivity versus pressure curve was depicted in Figure S9.

It can be observed that when the pressure was in small range, the S_R curve was closer to the S_ρ curve and far from the S_G curve. However, as the pressure increases, the S_R curve began to deviate from S_ρ curve and approached the S_G curve. The results indicated that the sensitive mechanism was related to the magnitude of the applied pressure. When the pressure was in small range, the sensitive mechanism was mainly based on piezoresistive effect, because there were fewer conductive paths, so the resistivity was sensitive to pressure. As the pressure increased, the carbon spheres contacted each other, causing the sensitivity of the resistivity to the pressure decreases sharply, and the sensitive mechanism was converted into a strain mechanism of the composite film. The piezoresistive effect and the deformation effect were declined due to the increase of the pressure, resulting in a decrease of the sensitivity.

4. Supporting Figures

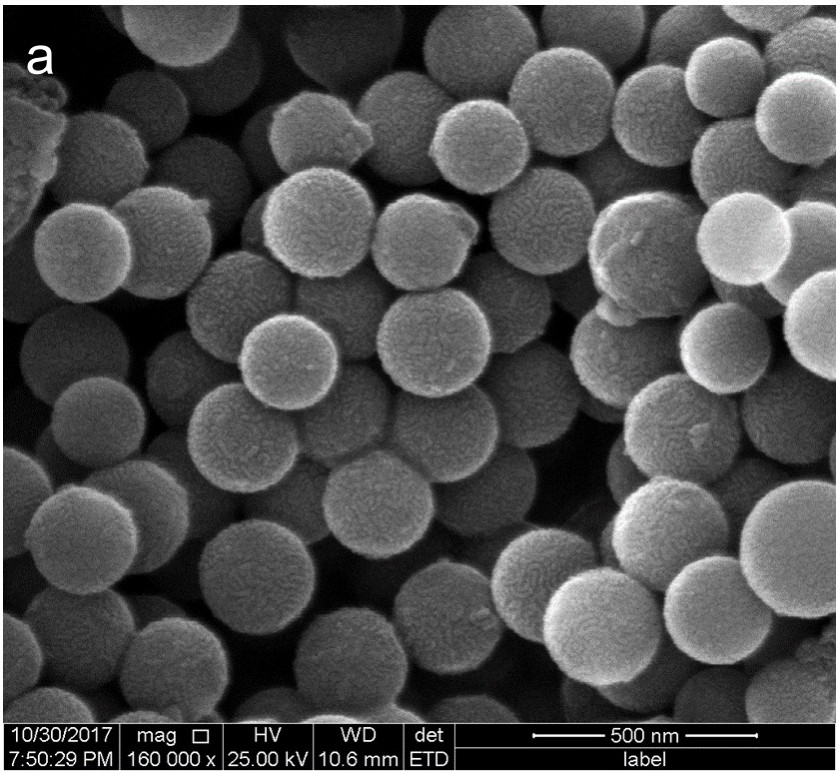

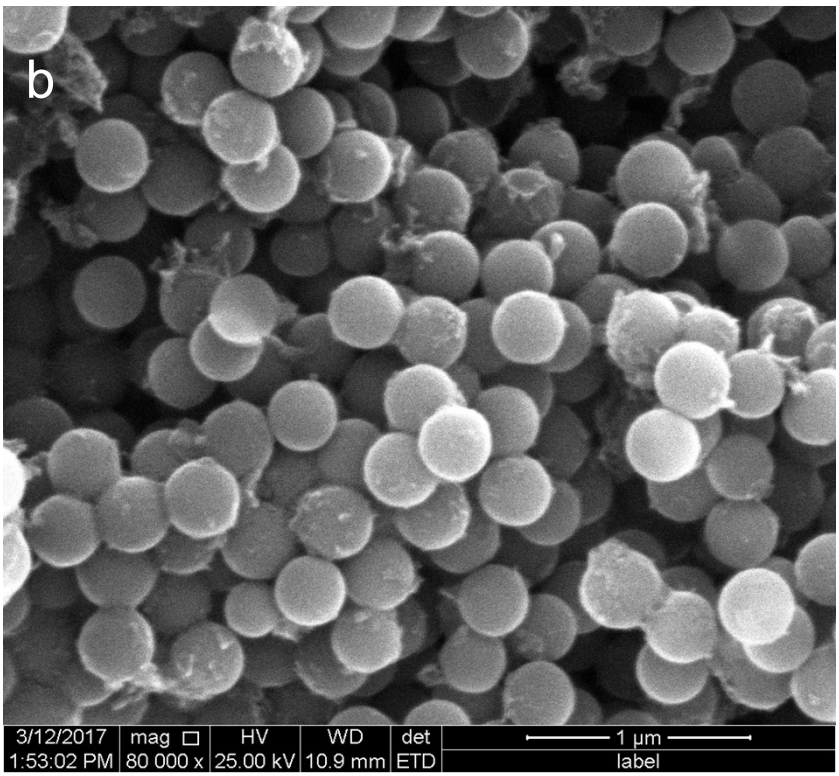

Supplementary Fig S1. The SEM image of HCSs and HCS-*g*-COOH. (a) HCSs; (b) HCS-*g*-COOH.

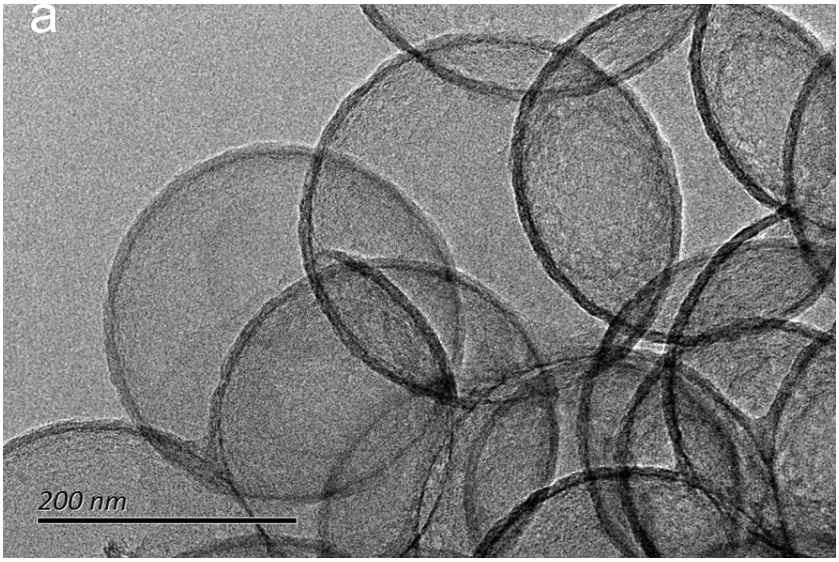

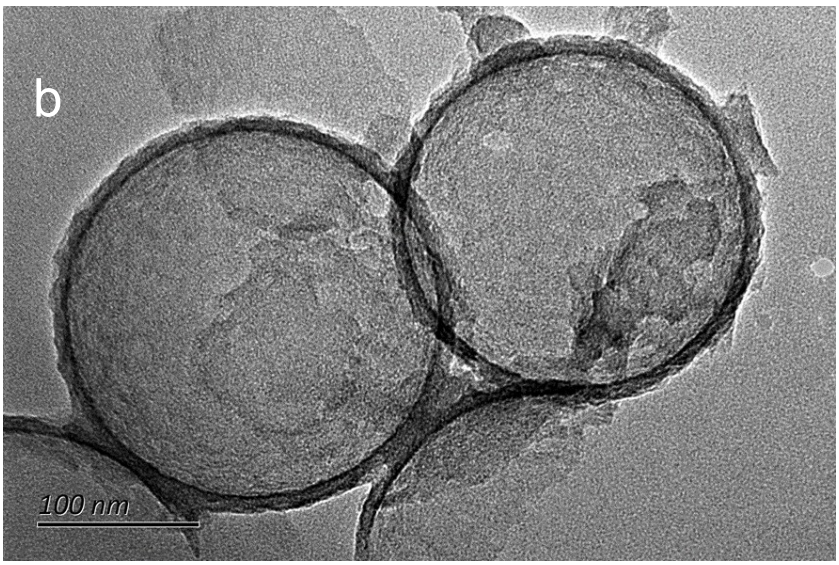

Supplementary Fig S2. The TEM image of HCSs and HCS-*g*-COOH. (a) HCSs; (b) HCS-*g*-COOH.

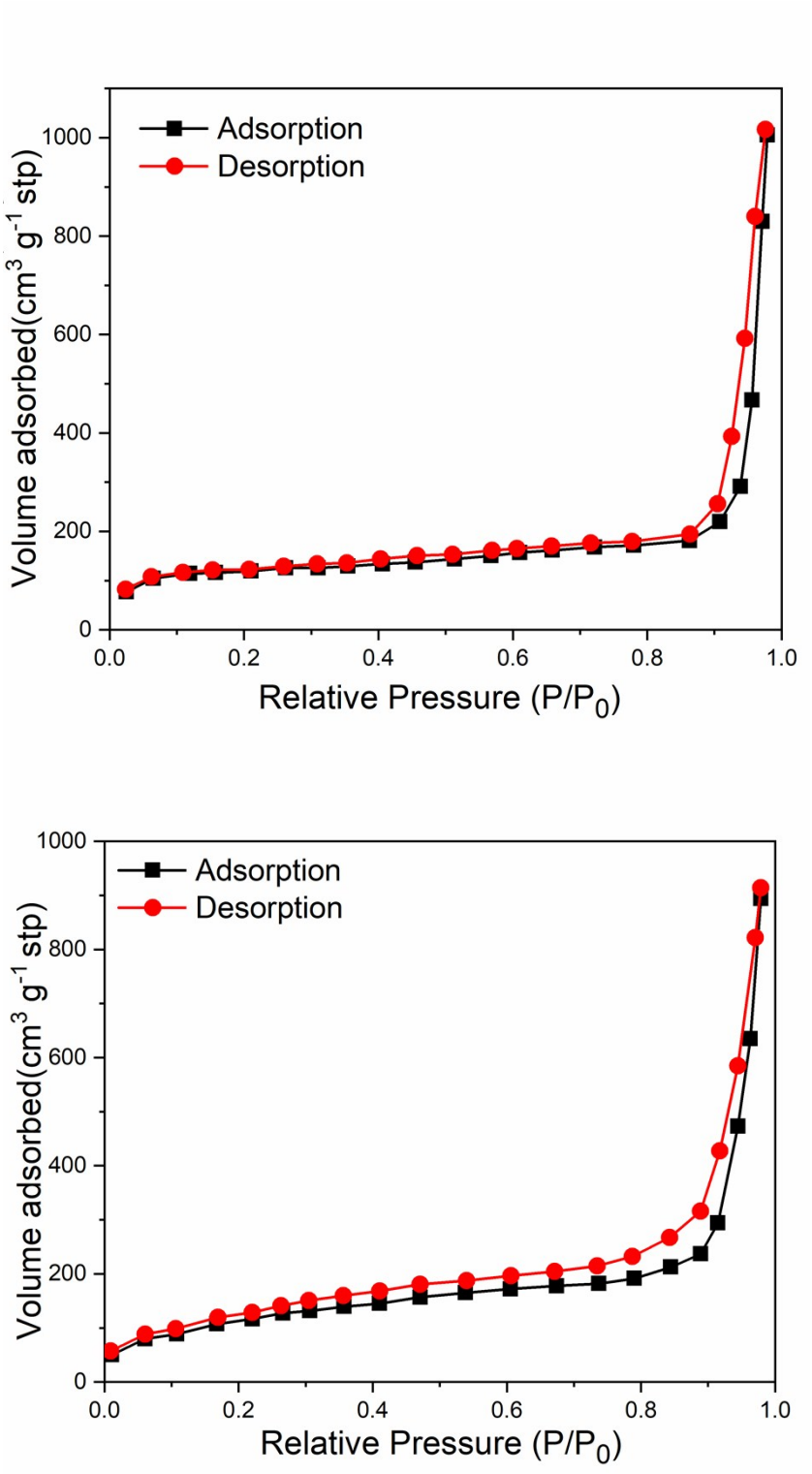

Supplementary Fig S3. Nitrogen adsorption−desorption isotherms and pore size distribution of HCSs and HCS-*g*-COOH

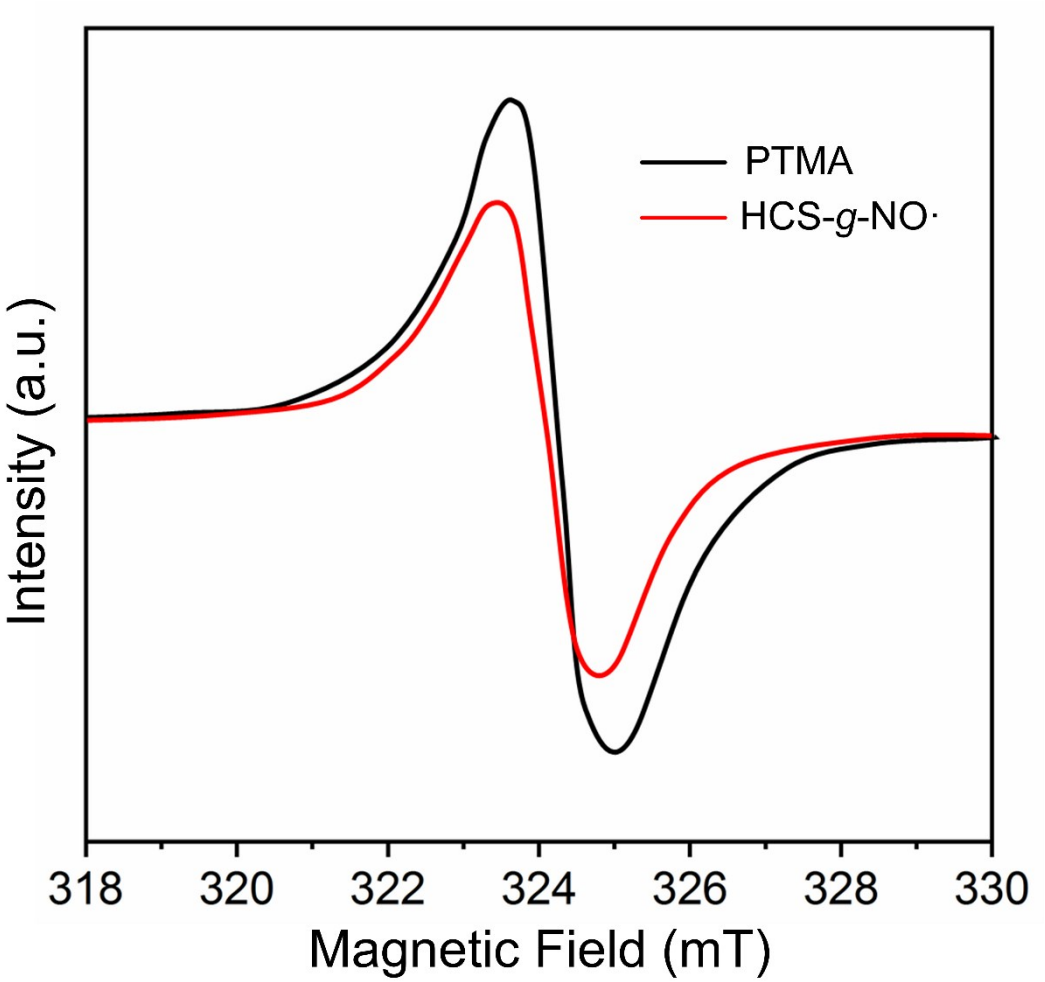

Supplementary Fig S4. The electron spin resonance (ESR) spectroscopy of PTMA and HCS-*g*-NO· ·

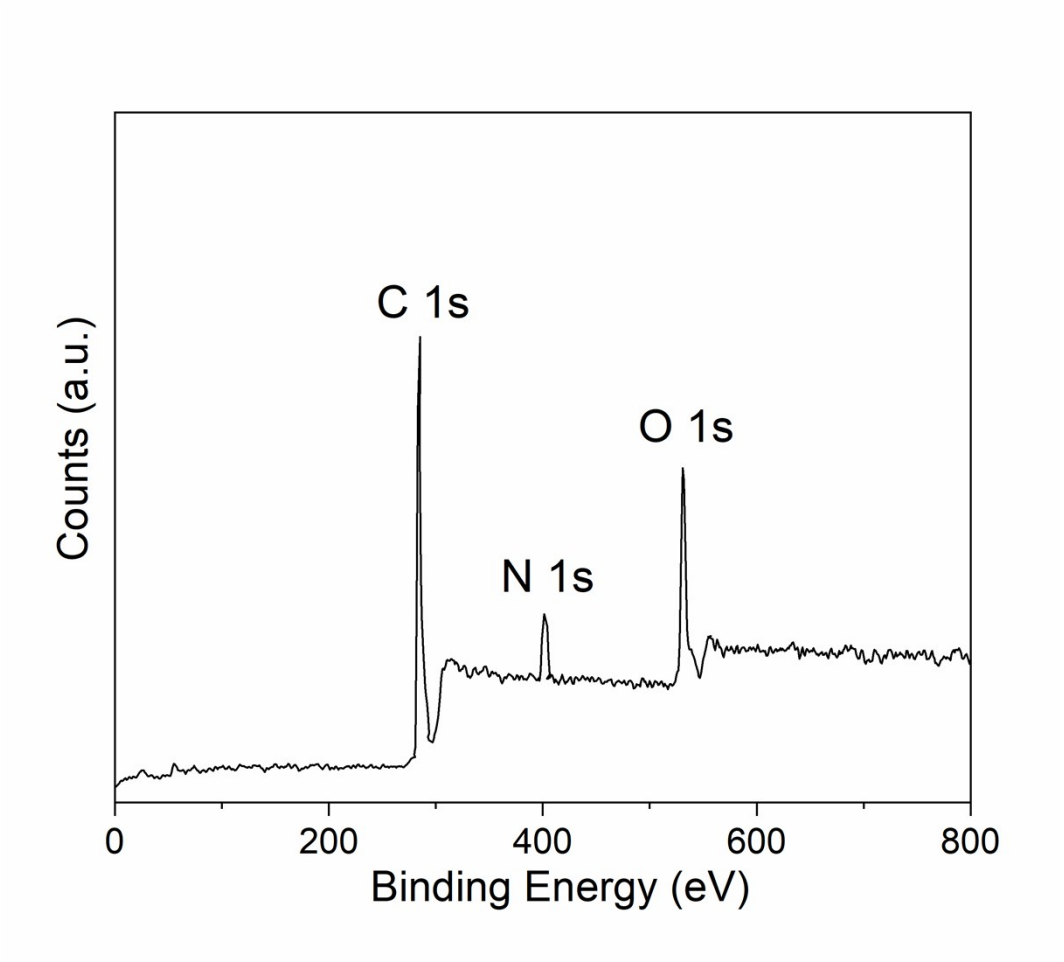

Supplementary Fig S5. The XPS total spectrum of HCS-*g*-NO·.

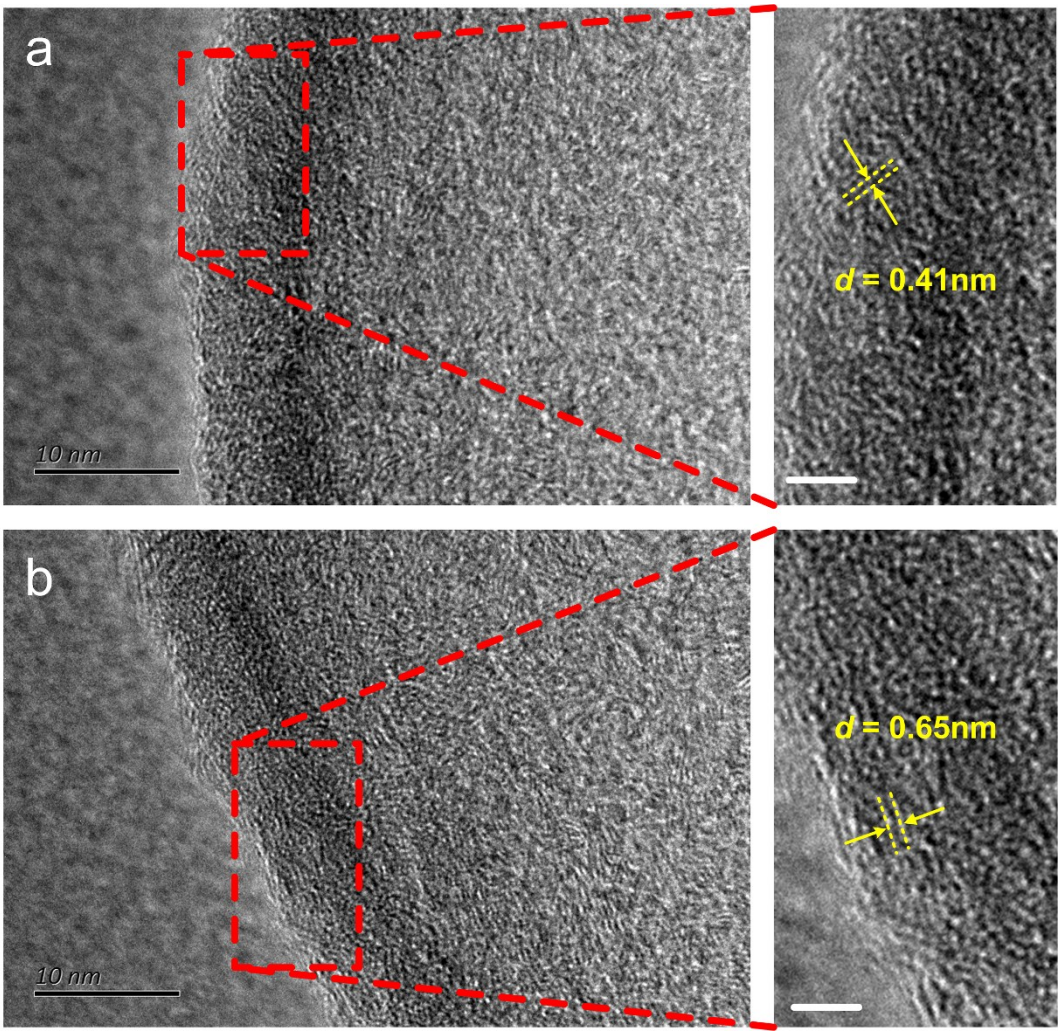

Supplementary Fig S6. The HRTEM of HCS-*g*-COOH and HCS-*g*-NO·, (a) HCS-*g*-COOH, (b) HCS-*g*-NO·. Red boxes show the enlarged morphology of the selected regions marked in (a) and (b); scale bar, 2 nm.

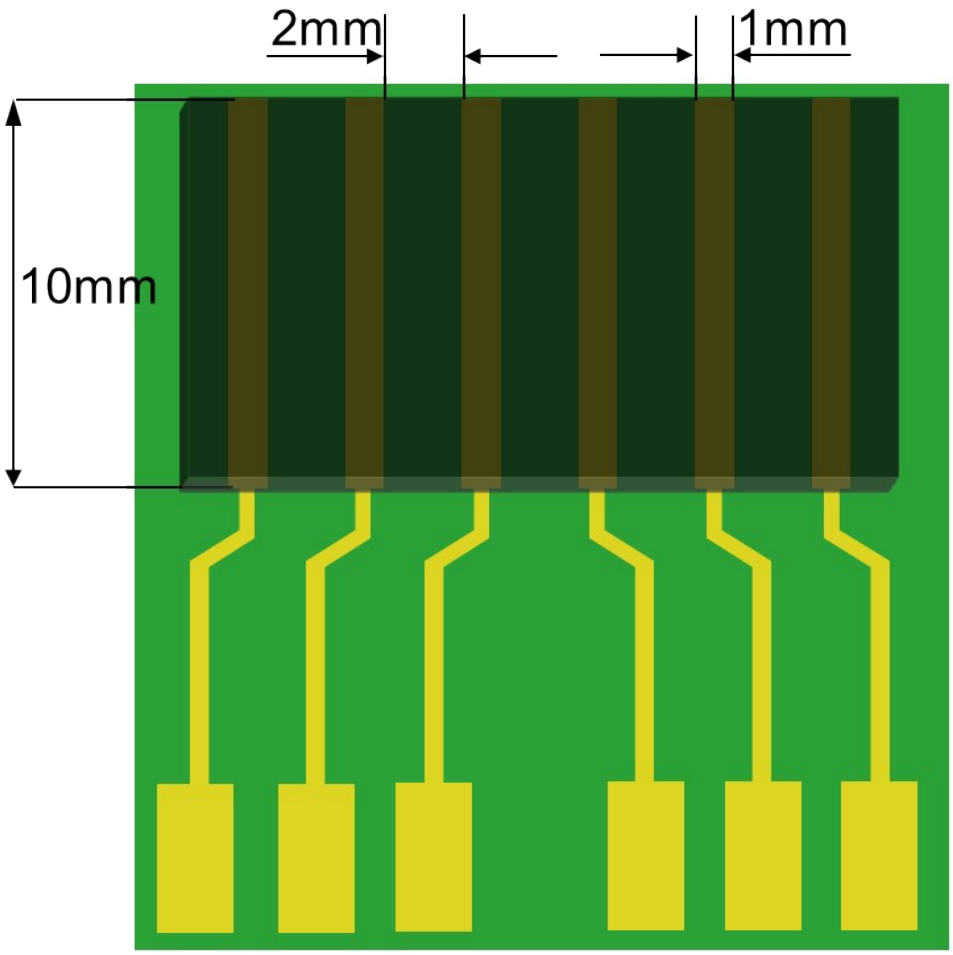

Supplementary Fig S7. Schematic diagram of composite resistivity test sample

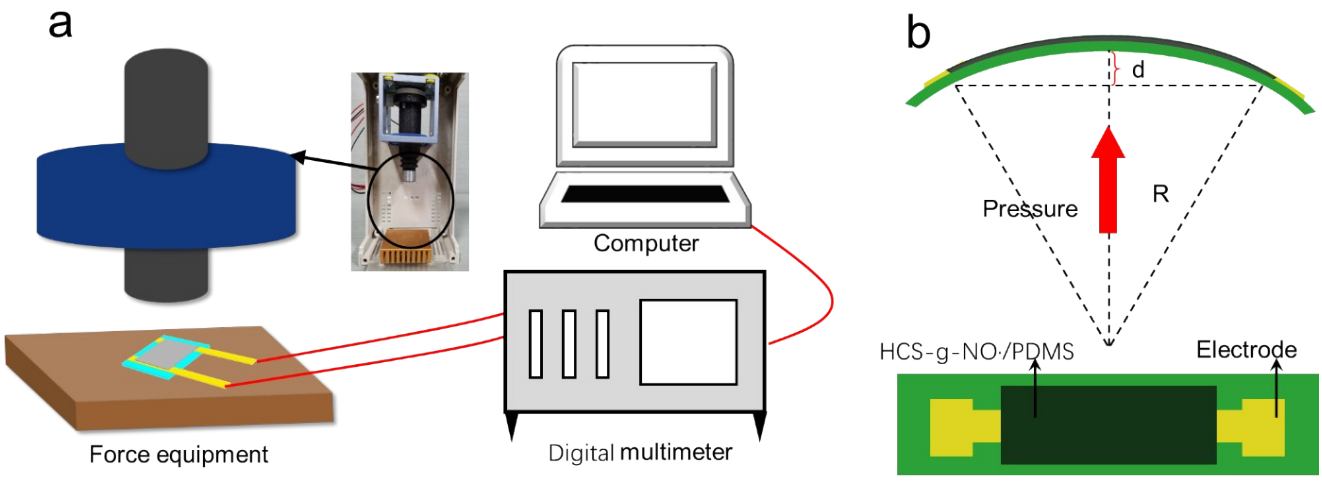

Supplementary Fig S8. Schematic diagram of sensing measurements

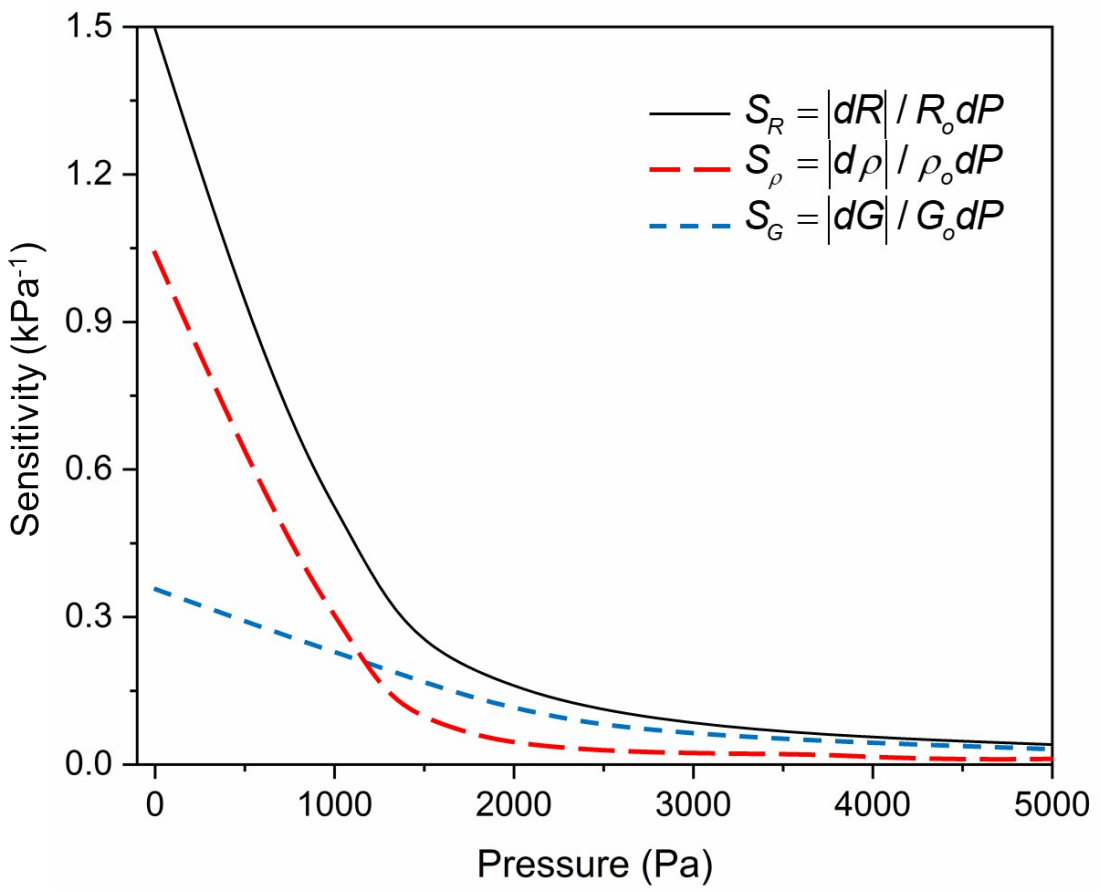

Supplementary Fig S9. Sensitivity curve of the sensor

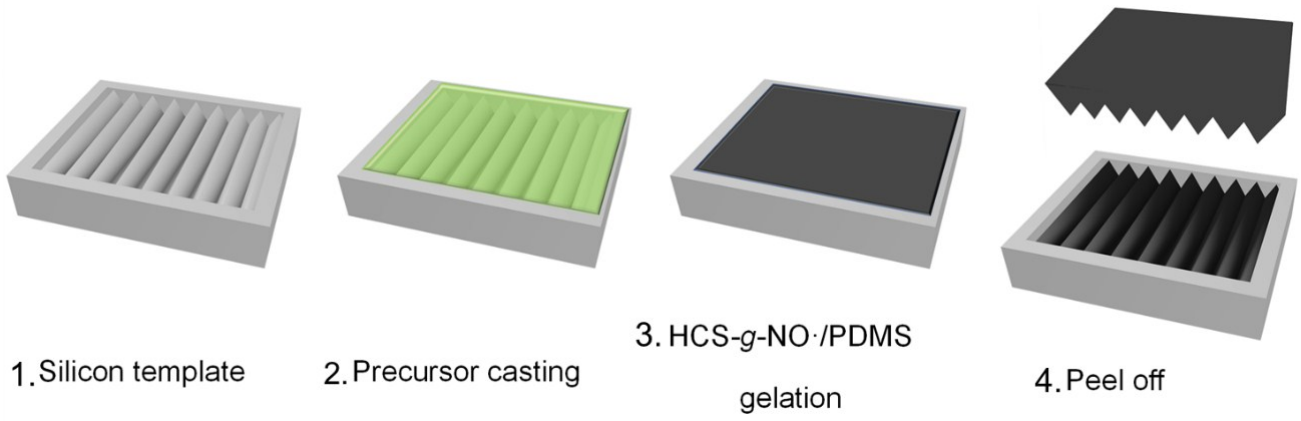

Supplementary Fig S10. Schematic process for the fabrication of micropatterned HCS-*g*-NO·/PDMS film

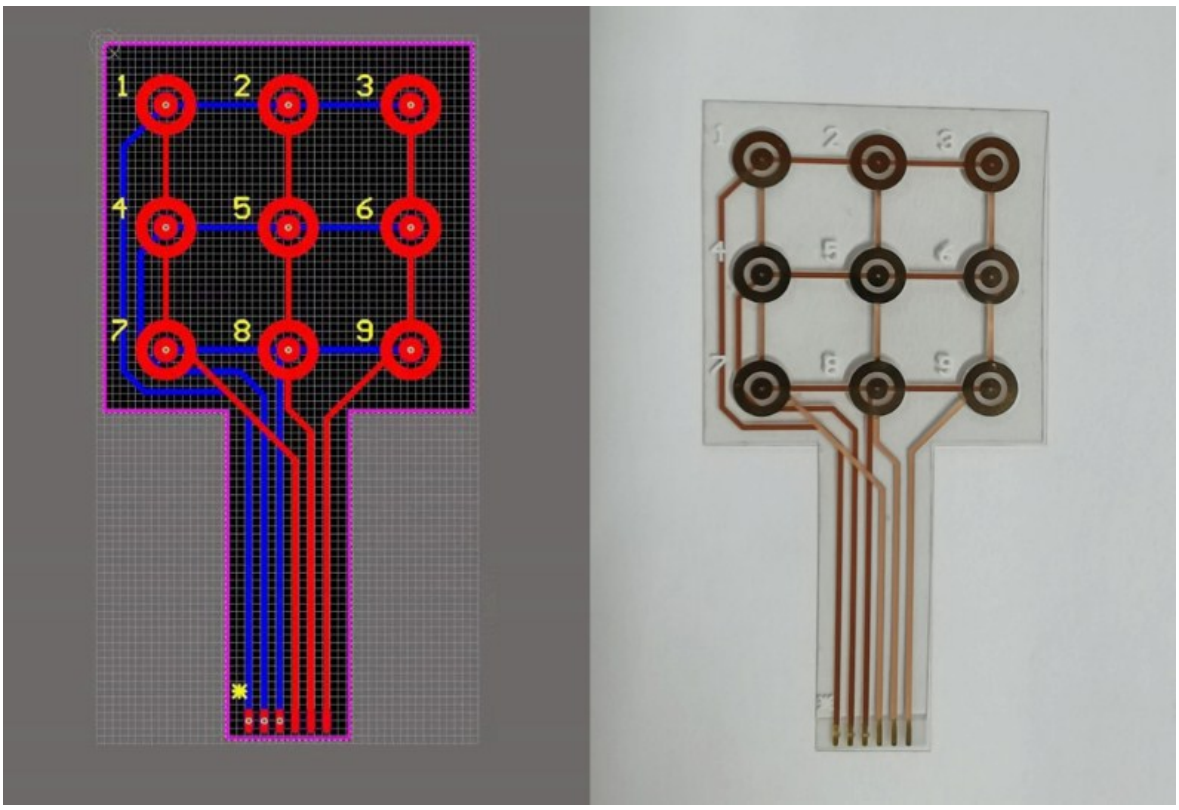

Supplementary Fig S11. Single-sided array electrode. Left: Electrode wiring connection diagram; right: array electrode digital photo

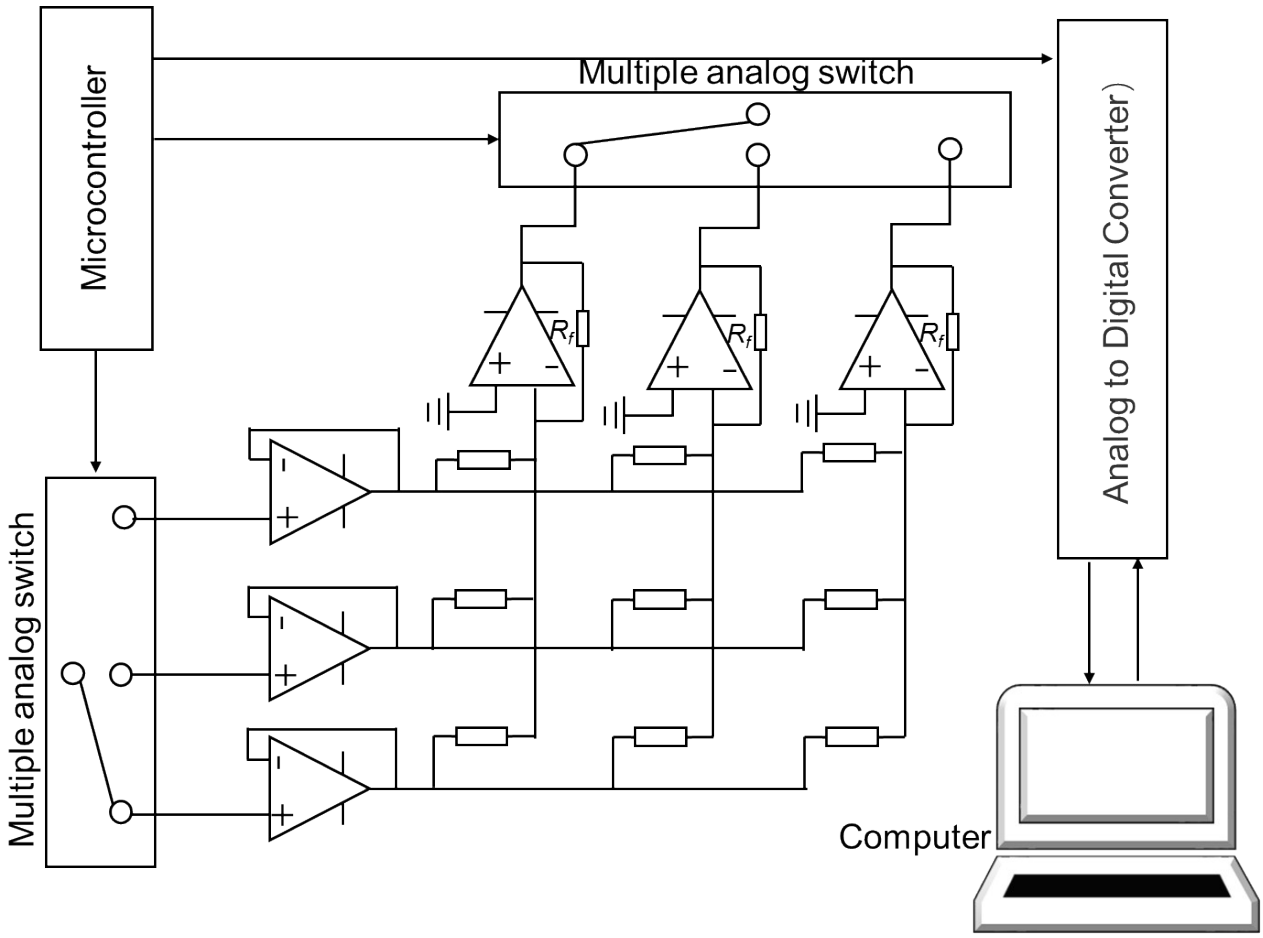

Supplementary Fig S12. Readout circuit schematic

References

1 B. Liu, D. Jia, and, Q. Meng, J. Rao, *Carbon*, 2007, **45**, 668–689.
2 J. Liu, M. Shao, Q. Tang, X. Chen, Z. Liu, Y. Qian, *Carbon,* 2003, **41**, 1682-1685.
3 L. Xu, W. Zhang, Q. Yang, Y. Ding, W. Yu, Y. Qian, *Carbon*, 2005, **43**, 1090-1092.
4 Y. Gu, L. Chen, Z. Li, Y. Qian, W. Zhang, *Carbon*, 2004, **42**, 235-238.
5 G. Zhang, Y. Xu, W. Lin, J. Wang, K. Yun and X. Sun, *Sci. China Mater.*, 2015, **58**, 534-542.
6 D. B. Xiong, X. F. Li, H. Shan, B. Yan, L. T. Dong, Y. Cao, D. J. Li, *J. Mater. Chem. A*, 2015, **3**, 11376-11386.
7 L. Yongye, L. Yanguang, W. Hailiang, Z. Jigang, W. Jian, R. Tom and D. Hongjie, *Nat. Mater.*, 2011, **10**, 780-786.
8 L. Yongye, W. Hailiang, Z. Jigang, L. Yanguang, W. Jian, R. Tom and D. Hongjie, *J. Am. Chem. Soc.*, 2012, **134**, 3517-3523.
9 D. C. Marcano, D. V. Kosynkin, J. M. Berlin, S. Alexander, S. Zhengzong, S. Alexander, L. B. Alemany, L. Wei and J. M. Tour, *Acs Nano*, 2010, **4**, 4806.
10 W. Gao, L. B. Alemany, L. Ci and P. M. Ajayan, *Nat. Chem.*, 2009, **1**, 403-408.
11 Z, Liu, J. T, Robinson, X. M, Sun, H. J. Dai, *J. Am. Chem. Soc.,* 2008, **130**, 10876–10877.
12 D. Yan, Y. Li, D. Jing, M. Lang and X. Huang, *J. Polym. Sci. Pol. Chem.*, 2011, **49**, 4747-4755.
13 W. Liu, Z. Chen, G. Zhou, Y. Sun, H. R. Lee, C. Liu, H. Yao, Z. Bao, Y. Cui, *Adv. Mater.*, 2016, **28**, 3578-3583.
14 J. Yin, P. Hu, J. Luo, L. Wang, M. F. Cohen and C. J. Zhong, *ACS Nano*, 2011, 5, 6516-6526.
15 D. S. Mclachlan, *Phys(C):Solid State Phys* ., 1987, **C20**, 865-875.